Catalysis
Science &
Technology

rsc.li/catalysis

ROYAL SOCIETY
OF **CHEMISTRY**
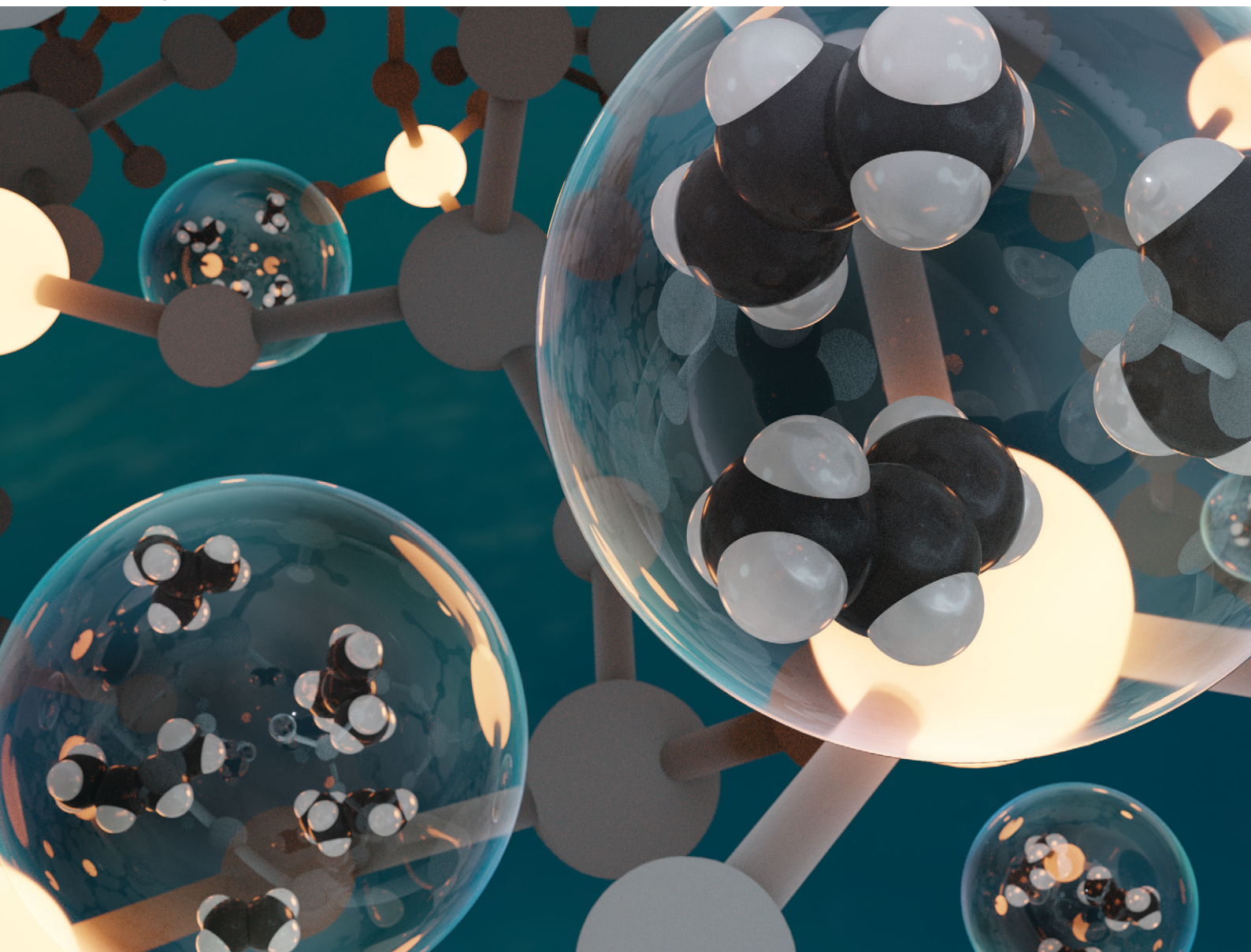
PAPER
Shinya Kokuryo, Koji Miyake *et al.*
Selective recovery of light olefins from polyolefin catalyzed
by Lewis acidic Sn-Beta zeolites without Brønsted acidity

Check for updates

Selective recovery of light olefins from polyolefin catalyzed by Lewis acidic Sn-Beta zeolites without Brønsted acidity†

Shinya Kokuryo,*[a] Kazuya Tamura,[a] Soshi Tsubota,[a] Koji Miyake, [iD] *[ab] Yoshiaki Uchida, [iD] [a] Atsushi Mizusawa,[c] Tadashi Kubo[c] and Norikazu Nishiyama[ab]

Recovering valuable products from waste materials has been critical in saving limited fossil resources. This study investigated the effects of the acid type in zeolites on the yields of light olefins during the catalytic cracking of polyolefins. Brønsted acid sites in zeolites promote the oligomerization of olefins *via* protonation, decreasing the light olefin yield. We prepared Lewis acidic Sn-Beta zeolites without Brønsted acids using a dealumination procedure. Sn-Beta zeolites exhibited a higher yield of light olefins (45%) than the pristine Beta zeolite (24%) on low-density polyethylene cracking. Our experiments revealed that Lewis acid sites promote light olefin production, and the absence of Brønsted acid sites dramatically inhibited the consecutive reactions, thereby increasing the light olefin yields. This study provides a new guideline for controlling the product distribution of polyolefin catalytic cracking.

1. Introduction

Carbon neutrality and sustainable development goals (SDGs) have been global trends,[1,2] and the development of recycling methods for some waste materials has been desired to realize a circular society.[3] Chemical recycling of plastic waste has been one important topic.[4–7] In chemical recycling, plastic wastes can be converted into valuable products such as monomers or petrochemical feedstocks, leading to the recycling of limited fossil resources.[8–12] Solid acid catalysts enable relatively selective production of gaseous products from polymer, while liquid products are mainly produced in thermal cracking (noncatalytic).[13–18] Zeolites are the most effective catalysts, and numerous studies have been conducted on the catalytic cracking of plastics using zeolites.[19–21] Zeolites are multifunctional solid acid catalysts with high hydrothermal stability.[22] One important feature of zeolites is shape selectivity derived from their uniform micropores.[23–25] Diffusivity can be controlled by changing the zeolitic pore size, depending on the molecular size of reactants and products.[26] Moreover, zeolites exhibit excellent

acidities. Zeolites are mainly composed of tetrahedral SiO_2, and a part of the Si^{4+} is substituted for Al^{3+}, leading to negatively charged sites accompanied by counter cations to balance the total charge.[27,28] Brønsted acid sites are generated by exchanging the counter cations with H^+. In addition, silanol groups and open Al sites (extra-framework- and -associated Al sites) serve as Lewis acid sites.[29–31] These abilities allow zeolites to decompose plastics at a lower temperature and control the product distribution compared to thermal cracking without catalysts.[32,33]

To date, most studies have focused on Brønsted acids, as the cracking reaction of the polymer has been assumed to proceed *via* Brønsted acids,[34,35] and the importance of Lewis acids has not been understood. However, our previous research revealed that Lewis acid sites also promote polymer cracking and decrease the decomposition temperature.[36,37]

To recycle the limited fossil resources, high-value products (*e.g.*, light olefins and aromatics) should be produced selectively from polyolefin cracking. In particular, light olefins are important raw materials for producing polymers and various chemicals.[38,39] Although product distributions can be controlled to some extent depending on the zeolitic framework type, and the yields of light olefins can be increased using zeolites with appropriate framework,[40] the control of micropore structure is reaching its limits. In this study, we focused on the mechanism of the catalytic cracking of polyolefins and aimed to increase the yields of light olefins using a chemical approach.

Unlike the radical mechanism of thermal cracking, the catalytic cracking of polyolefins proceeds *via* a carbenium ion

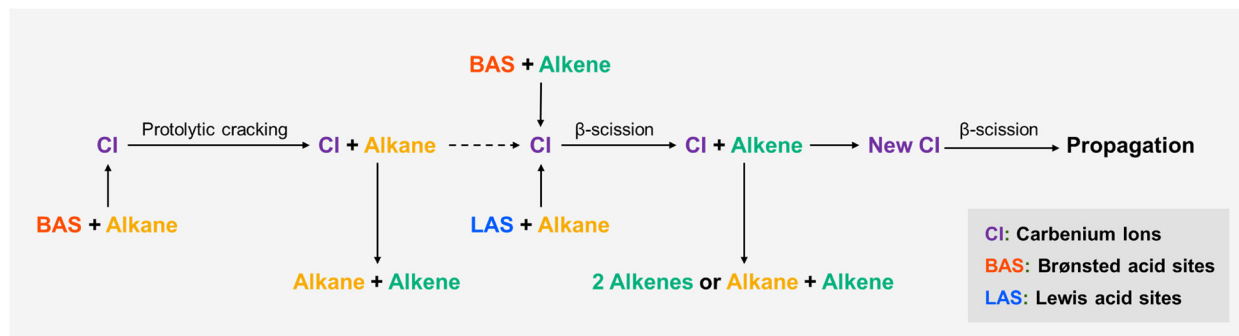*[a] Division of Chemical Engineering, Graduate School of Engineering Science, Osaka University, 1-3 Machikaneyama, Toyonaka, Osaka 560-8531, Japan. E-mail: skokuryo@cheng.es.osaka-u.ac.jp, kojimiyake@cheng.es.osaka-u.ac.jp*
[b] Innovative Catalysis Science Division, Institute for Open and Transdisciplinary Research Initiatives (ICS-OTRI), Osaka University, Suita, Osaka 565-0871, Japan
[c] AC Biode Co., Ltd., 498-6 Iwakura Hanazono, Sakyo, Kyoto, 606-0024, Japan
† Electronic supplementary information (ESI) available. See DOI: https://doi.org/10.1039/d4cy00317a

This journal is © The Royal Society of Chemistry 2024

Catal. Sci. Technol., 2024, **14**, 3589–3595 | 3589

Scheme 1 Reaction mechanism of the catalytic cracking of polyolefins on zeolite acid sites.

mechanism, as shown in Scheme 1.[35] Brønsted and Lewis acids produce the carbenium ions *via* protonation and abstraction of a hydride ion, respectively. These carbenium ions are converted into shorter hydrocarbon chains *via* β-scission.

Brønsted acid sites promote the protonation of olefins, thereby converting light olefins into other hydrocarbon materials *via* hydrogen transfer, oligomerization, isomerization, and cracking. Thus, zeolites have been used as catalysts for the conversion of light olefins.[41–43] Therefore, in the catalytic cracking of polymers, a decrease in the number of Brønsted acid sites is assumed to lead to an increase in the yield of light olefins. J. Lee *et al.* prepared lanthanum-containing zeolites and investigated the relationship between basicity and product distribution in C5 raffinate cracking.[44] La species decrease the Brønsted acidity by covering the sites and increasing the basicity, increasing the selectivity for light olefins (ethylene and propylene). However, the decrease in Brønsted acidity and porosity by La-loading causes a decrease in catalytic activity and conversion of C5 raffinate; therefore, loading a solid base to zeolites is unsuitable for the catalytic cracking of polymers. As mentioned above, not only Brønsted acids but also Lewis acids promote the catalytic cracking of polymers. Therefore, we dealuminated zeolite Beta and incorporate Sn into the framework to prepare zeolites with only Lewis acids. The effect of Lewis acids and the absence of Brønsted acids on the yields of light olefins during low-density polyethylene (LDPE) cracking was examined.

2. Experimental

2.1. Catalyst preparation

Sn-Beta zeolites were synthesized according to previous literature.[45] First, the dealumination of Beta zeolites was conducted as a pretreatment for the synthesis of Sn-Beta. Commercial H$^+$-type Beta zeolites obtained from TOSOH (SiO$_2$/Al$_2$O$_3$ = 28.9) and 35 wt% HNO$_3$ solution obtained from Wako FUJIFILM were mixed at a mass ratio of 1/9, placed in a Teflon-sealed autoclave, and then heated at 180 °C for 24 h. The obtained powder was washed with deionized water by filtration until its pH was neutral and dried overnight at 90 °C to obtain deAl-Beta.

To prepare precursor solution for Sn-Beta, 35 wt% TEAOH solution (Wako FUJIFILM), SnCl$_4$·5H$_2$O (Wako FUJIFILM), and deionized water were mixed to a concentration of 0.2 mol L^{-1} and 0.016 mol L^{-1} for TEAOH and Sn, respectively. An appropriate amount of precursor solution was added to the prepared deAl-Beta (0.5 g) to a mass ratio of Sn/Beta = x/100 (x = 2, 4, 6). The mixture was then placed in a Teflon-sealed autoclave and heated at 140 °C for 24 h. The obtained powder was washed by centrifugation with deionized water thrice, dried at 90 °C overnight, and then calcined at 550 °C for 6 h. The synthesized zeolites were named Sn-Beta(x).

2.2. Characterization

The crystal structures of all the products were characterized by X-ray diffraction (XRD) patterns measured on a PANalytical X'Pert-MPD diffractometer using Cu-Kα radiation. The morphologies of the samples were observed by transmission electron microscopy (TEM). Energy-dispersive X-ray spectroscopy (EDS) was performed to determine the Sn content using a JEOL JCM-7000 instrument. To obtain physical information about the samples, N$_2$ adsorption measurements were conducted at −196 °C using a BELSORP-Max instrument (MicrotracBel). Before the N$_2$ adsorption measurements, the samples were heated to 250 °C for 3 h under vacuum. The diffuse reflectance ultraviolet-visible (UV-vis) spectra of the samples were recorded using a JASCO V-770 spectrophotometer. Fourier-transform infrared (FT-IR) spectra of the pyridine-adsorbed samples were measured using a mercury-cadmium-telluride (MCT) detector with an average of 128 scans at a resolution of 4 cm^{-1} in the wavenumber range 4000–400 cm^{-1}. Prior to FT-IR spectroscopy, pyridine was adsorbed onto the samples, which were then purged with He at 150 °C for 15 min to remove excess pyridine. NH$_3$ temperature programmed desorption (NH$_3$-TPD) using a BELCAT II equipped with a quadrupole mass spectrometer (MicrotracBEL) was used to evaluate the acid strength of zeolites.

2.3. LDPE catalytic cracking

The zeolites and LDPE powder were mixed in a mass ratio of zeolite/LDPE = 1/4. The catalytic activities of the zeolites for LDPE cracking were evaluated by thermogravimetric (TG)

analysis using a DTG-60A (SHIMADZU). The mixture was heated to 600 °C at a heating rate of 5 °C min^{-1} under a N$_2$ flow (60 ml min^{-1}), and the cracking temperature was determined. The product distributions were analyzed using gas chromatography. The zeolite/LDPE mixture was placed in an aluminum pan with an inner diameter of 24 mm and heated to 600 °C at a rate of 5 °C min^{-1} under N$_2$ flow (60 ml min^{-1}). The exit gas generated during the reaction was collected in a gas bag using a cold trap with ice water. The mass increase of the trap after the reaction was taken as the mass of the solid and liquid products and their yields (Y_{S+L}) were calculated on a mass basis. The amount of coke deposited was evaluated using TG at a heating rate of 5 °C min^{-1} under air and their yields (Y_C) were also calculated on a mass basis. The weight loss from 350 to 600 °C was attributed to the combustion of the deposited coke. The yields of gaseous products (Y_G) were calculated by the following equation: $Y_G = 100 - (Y_{S+L} + Y_C)$. The yield of each gas product was analyzed using a Shimadzu GC-2025 gas chromatograph equipped with a flame ionization detector and the yields of light olefins (Y_{LO}) were calculated by the following equation: $Y_{LO} = Y_G(X_{C_2H_4} + X_{C_3H_6} + X_{C_4H_8})$. Here, X is the selectivity of each product.

2.4. Isobutene conversion tests

Isobutene conversion reactions were conducted in a fixed-bed reactor at atmospheric pressure. The catalysts were placed in a quartz tube with an inner diameter of 4 mm and then heated to a certain temperature under He flow. The feed gas of 9.6 vol% isobutene and balanced He was fed at $F_{total} = 1.66$ cm^3 min^{-1} and the contact time was $W/F = 116.8$ g h mol^{-1}. The products were analyzed online using Shimadzu GC-2025 gas chromatographs equipped with a flame ionization detector.

3. Results & discussion

The XRD patterns of all samples showed peaks derived from the Beta structure centered at approximately 8° and 23°,[46,47] as shown in Fig. 1, indicating that zeolites maintained their structure even through dealumination and the Sn-incorporation procedure. Moreover, no peaks derived from impurities such as bulk SnO$_2$ species were detected, indicating that almost all Sn species were incorporated into the zeolite framework.

EDS analysis was conducted to evaluate the composition of the zeolites (Table 1). After the dealumination procedure, the Al content was below the detection limit, indicating that the Al species in the zeolites were almost completely removed. The Sn content of the samples increased with increasing Sn content in the preparation solution. The morphologies of the samples were investigated by TEM (Fig. S1†). The acid treatment partly disrupted the zeolite structure, thereby deAl-Beta had a ragged surface. Moreover, the Sn incorporation procedure smoothened the surface of the zeolites because the procedure was performed under
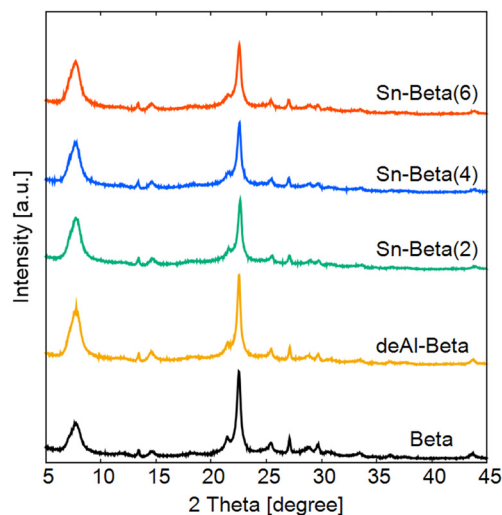

Fig. 1 XRD patterns of Beta, deAl-Beta, and Sn-Beta(x).

strong basic conditions and the SiO$_2$ framework was partly dissolved. The porosities of the catalysts were evaluated by N$_2$ adsorption. The pore volume of deAl-Beta was lower than that of the pristine Beta because of the decrease in its crystallinity, as shown in Fig. S2.† Moreover, Sn incorporation decreased the zeolite micropore volume, suggesting that the zeolite framework was partly dissolved and amorphous SiO$_2$ occluded the zeolitic micropore, which is consistent with the changes observed in the TEM images.

The detailed chemical states of the Sn species in the synthesized zeolites were investigated using UV-vis spectroscopy. A reference SnO$_2$ has a broad absorbance band at 210–280 nm,[48] while all Sn-Beta samples have sharp peaks at 206 nm[49] derived from charge transfer between O and isolated tetrahedral Sn^{4+}, as shown in Fig. 2, indicating that Sn was incorporated into the zeolite frameworks. However, Sn-Beta(6) showed a slight peak at around 280 nm, indicating that the excess amount of Sn existed as extra-framework species.

Moreover, the intensity of the absorption band increases with increasing Sn content. The acidity of the samples was investigated by FT-IR spectroscopy using pyridine as a probe molecule (Fig. 3). Pyridine is a basic molecule that adsorbs on the acid sites of zeolites in various forms depending on the acid type. Therefore, the acidity of zeolites can be evaluated separately for each acid type. A peak at 1545 cm^{-1} derived from pyridine adsorbed on Brønsted acid sites[50] was not observed, indicating that no Brønsted acid sites were

Table 1 Si/Al and Si/Sn ratio of Beta, deAl-Beta, and Sn-Beta(x)

	Si/Al	Si/Sn
Beta	12.24	—
deAl-Beta	∞	—
Sn-Beta(2)	∞	492
Sn-Beta(4)	∞	130
Sn-Beta(6)	∞	119
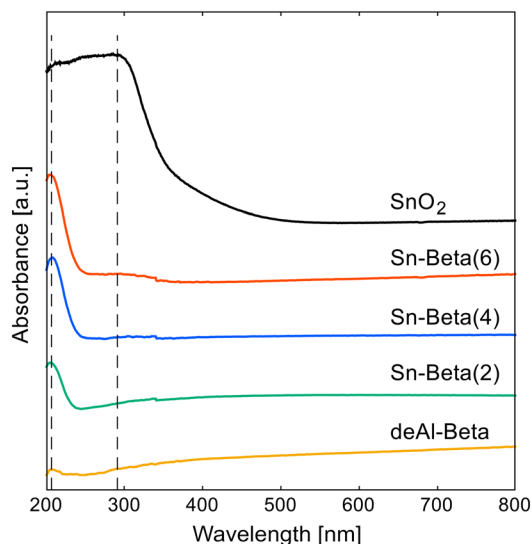
Fig. 2 UV-vis spectra of Beta, Sn-Beta(*x*), and SnO$_2$.

Fig. 4 TG curves obtained during catalytic cracking of LDPE with Beta, daAl–Beta, and Sn–Beta(*x*).

present in the dealuminated samples. A peak at 1445 cm^{-1} corresponding to hydrogen-bonded pyridine[50] was observed in deAl-Beta, indicating that the number of silanol groups increased by dealumination. Moreover, for Sn-Beta samples, peaks of coordinated pyridine on the Lewis acid sites (1450 cm^{-1})[50] were observed, and the intensity of the peak became strong with the increase in the Sn content, indicating that the incorporated Sn species serve as Lewis acid sites. Additionally, NH$_3$-TPD measurements revealed that Sn-Beta samples had strong Lewis acid sites derived from Sn sites (the peak top is 747 °C) as shown in Fig. S3.†

The activity of the samples in polyolefin cracking was evaluated by TG and GC using low-density polyethylene (LDPE) powder. First, the decomposition temperatures of LDPE with and without catalysts were measured by TG at a heating rate of 5 °C min^{-1} to 600 °C under a N$_2$ atmosphere.

The catalytic cracking of LDPE with Sn-Beta zeolites occurred at higher temperatures than that with pristine Beta zeolites because of the lack of active sites, as shown in Fig. 4. The Si/Sn ratio of Sn-Beta(6) is 119, while the Si/Al ratio of pristine Beta is approximately 12, as shown in Table 1; therefore, this difference in the number of acidic atoms led to an increase in the cracking temperature. However, the cracking temperature with Sn-Beta zeolites lowered with the increase in the Sn content, indicating that LDPE cracking was accelerated even by only Lewis acidity originating from Sn.

GC was used to analyze the product distribution during LDPE cracking with and without catalysts. First, the selectivities of gas, liquid + wax, and coke were calculated from a mass balance (Fig. 5a). The gas yield with pristine Beta was more than 80%, whereas that without catalysts was approximately 50%. In the case of deAl-Beta, the selectivity was almost the same as that of thermal cracking (noncatalytic). However, the gas yields increased to the same extent as in pristine Beta by the incorporation of Sn, indicating that Lewis acidic Sn sites promoted the cracking *via* the carbenium ion mechanism. Moreover, the amount of coke deposited on Sn-Beta zeolites was lower than that on pristine Beta, as shown in Fig. S4.† This is because the effect of the elimination of hydrogen transfer reaction that occurs at the Al sites, and the production of coke precursors such as aromatics was inhibited.[51,52] The detailed distributions of the gaseous products were analyzed using GC, as shown in Fig. 5b. The selectivity of C6+ products with pristine Beta was lower than 30%, whereas that without catalysts was approximately 70%, and the gaseous product distributions with deAl-Beta was almost the same as that of pristine Beta. These results indicate that silanol groups in zeolites served as Lewis acids and promoted LDPE cracking. Moreover, the selectivity of C4 and C5 products with Sn-Beta(6) was higher than that of other Sn-Beta samples, suggesting that an excess amount of Sn species such as extra-framework Sn also proceeded the LDPE cracking.
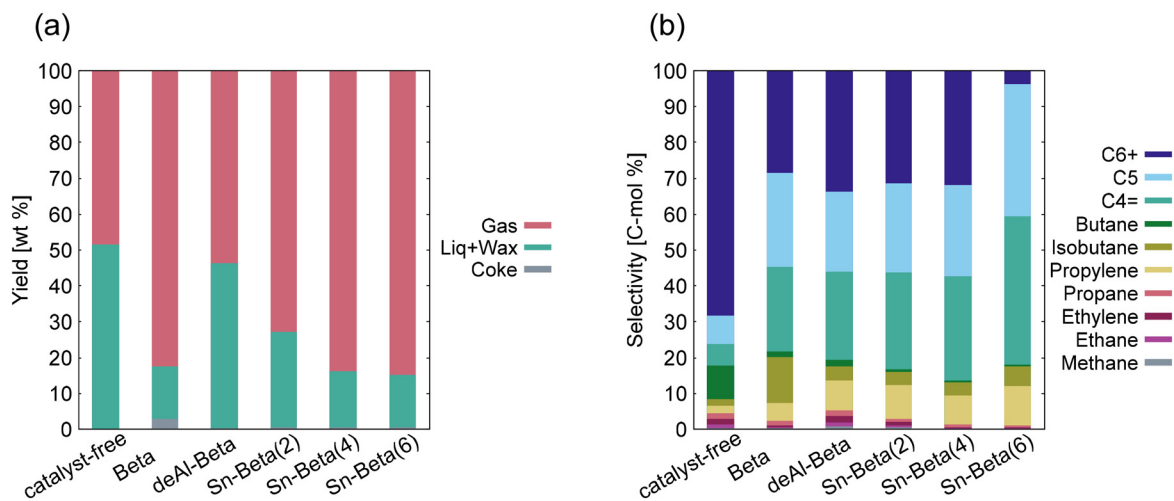

Fig. 3 FT-IR spectra of pyridine adsorbed on Beta, deAl-Beta, and Sn-Beta(*x*).

3592 | *Catal. Sci. Technol.*, 2024, **14**, 3589–3595

This journal is © The Royal Society of Chemistry 2024

Fig. 5 (a) Yields by group and (b) gas product distribution in catalytic cracking of LDPE with Beta, deAl-Beta, and Sn-Beta(x).

The selectivity for olefins and paraffins in C2–C4 products was calculated (Fig. 6a). The olefin selectivity was increased by dealumination because of the elimination of Brønsted acidity and further increased to nearly 90% by Sn incorporation. Moreover, the yields of light olefins increased by approximately 20% using Sn-Beta(6) compared to pristine Beta, as shown in Fig. 6b. These results indicate that the elimination of Brønsted acid sites leads to inhibition of olefin conversion in polyolefin catalytic cracking.

Finally, we conducted a light olefin conversion test with pristine Beta and Sn-Beta(6) using isobutene as a model reactant. The reaction temperature was determined from the TG results. Ty is defined as the temperature at which y% of LDPE was decomposed (y = 20, 50, 60) as shown in Fig. S5.† The isobutene conversion test was conducted at the determined Ty with a fixed-bed reactor, and the conversion was calculated by taking into account all C4 olefin products. In the case of pristine Beta, the conversions were approximately 90% and most of the product

was isobutane, indicating that the protonation of olefins by Brønsted acids was promoted (Fig. 7a). Meanwhile, the activity of Sn-Beta(6) for isobutene conversion was low, with a conversion rate of less than 40%, even though the reaction was conducted at higher temperatures than in the case of pristine Beta (Fig. 7b). Thus, the use of non-Brønsted acidic zeolites protects light olefins from conversion to other hydrocarbons.

4. Conclusions

In summary, Lewis acidic Sn-Beta zeolites recorded higher yields of light olefins (ethylene, propylene, and butene) than pristine Beta during LDPE catalytic cracking. Brønsted acids derived from the Al sites in zeolites promote the protonation of olefins, thereby converting light olefins into other hydrocarbon materials *via* hydrogen transfer, oligomerization, isomerization, and cracking. Therefore, during the cracking reaction, the produced light olefins were protected from being converted to
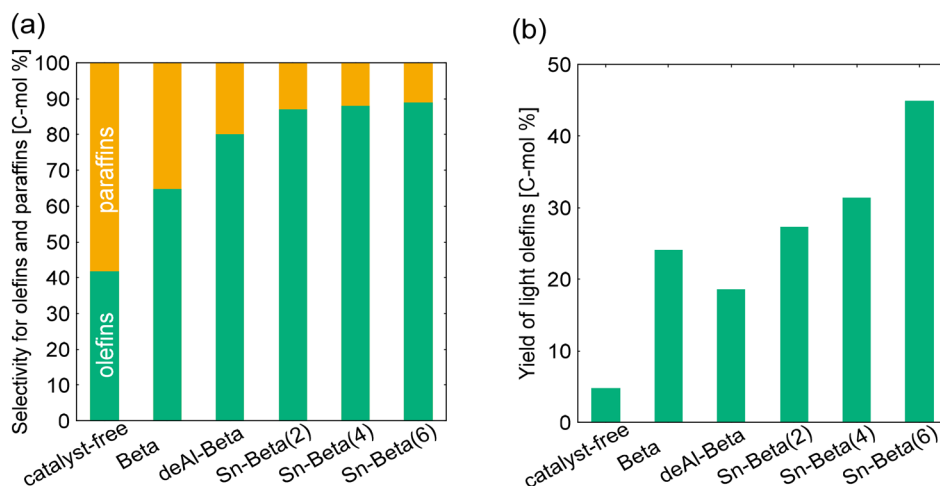

Fig. 6 (a) Selectivity for olefins and paraffins and (b) yield of light olefins in catalytic cracking of LDPE with Beta, deAl-Beta, and Sn-Beta(x).

This journal is © The Royal Society of Chemistry 2024

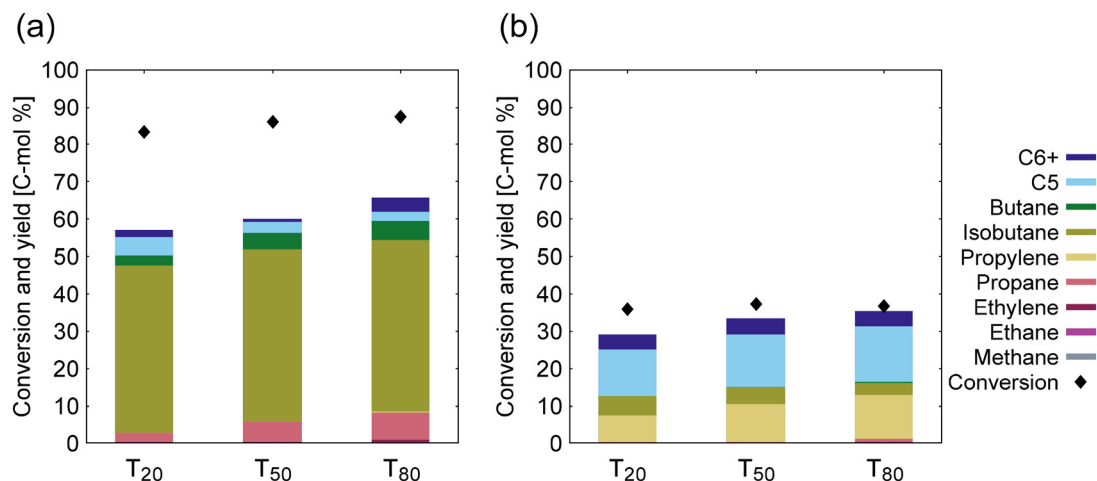*Catal. Sci. Technol.*, 2024, **14**, 3589–3595 | **3593**

Fig. 7 Isobutene conversion tests over (a) Beta and (b) Sn-Beta(6).

other hydrocarbons by the absence of Brønsted acid sites, leading to an increase in light olefin yields. Additionally, it was confirmed that the activity of Sn-Beta zeolites for light olefin conversion was significantly lower than that of pristine Beta using isobutene as a model reactant. This study provides a new method for controlling product distributions during the catalytic cracking of polyolefins.

Author contributions

Shinya Kokuryo: conceptualization, investigation, visualization, writing – original draft. Kazuya Tamura: investigation, writing – review & editing. Soshi Tsubota: investigation, writing – review & editing. Koji Miyake: conceptualization, supervision, visualization, methodology, writing – review & editing. Yoshiaki Uchida: writing – review & editing. Atsushi Mizusawa: writing – review & editing. Tadashi Kubo: writing – review & editing. Norikazu Nishiyama: supervision, resources, writing – review & editing.

Conflicts of interest

There are no conflicts to declare.

Acknowledgements

Notes and references

1 S. Yang, D. Yang, W. Shi, C. Deng, C. Chen and S. Feng, *Environ. Sci. Pollut. Res.*, 2022, **30**, 81725–81744.
2 J. G. Backes and M. Traverso, *Curr. Opin. Green Sustainable Chem.*, 2022, **38**, 100683.
3 W. Ferdous, A. Manalo, R. Siddique, P. Mendis, Y. Zhuge, H. S. Wong, W. Lokuge, T. Aravinthan and P. Schubel, *Resour., Conserv. Recycl.*, 2021, **173**, 105745.
4 T. Thiounn and R. C. Smith, *J. Polym. Sci.*, 2020, **58**, 1347–1364.
5 J.-P. Lange, *ACS Sustainable Chem. Eng.*, 2021, **9**, 15722–15738.
6 M. G. Davidson, R. A. Furlong and M. C. McManus, *J. Cleaner Prod.*, 2021, **293**, 126163.
7 L. Gan, Z. Dong, H. Xu, H. Lv, G. Liu, F. Zhang and Z. Huang, *CCS Chem.*, 2024, **6**, 313–333.
8 S. Nanda and F. Berruti, *Environ. Chem. Lett.*, 2021, **19**, 123–148.
9 A. Fivga and I. Dimitriou, *Energy*, 2018, **149**, 865–874.
10 K. Kumar Jha and T. T. M. Kannan, *Mater. Today: Proc.*, 2021, **37**, 3718–3720.
11 S. D. A. Sharuddin, F. Abnisa, W. M. A. W. Daud and M. K. Aroua, *IOP Conf. Ser.: Mater. Sci. Eng.*, 2018, **334**, 012001.
12 M. Crippa and B. Morico, in *Studies in Surface Science and Catalysis*, Elsevier, 2020, vol. 179, pp. 215–229.
13 M. V. Singh, S. Kumar and M. Sarker, *Sustainable Energy Fuels*, 2018, **2**, 1057–1068.
14 X. Lin, Z. Zhang, Z. Zhang, J. Sun, Q. Wang and C. U. Pittman, *Waste Manage.*, 2018, **79**, 38–47.
15 P. E. Nwankwor, I. O. Onuigbo, C. E. Chukwuneke, M. F. Yahaya, B. O. Agboola and W. J. Jahng, *Int. J. Energy Environ. Eng.*, 2021, **12**, 77–86.
16 S. Zhang, S. Zhu, H. Zhang, X. Liu and Y. Xiong, *Int. J. Hydrogen Energy*, 2019, **44**, 26193–26203.
17 L. S. Diaz-Silvarrey, A. McMahon and A. N. Phan, *J. Anal. Appl. Pyrolysis*, 2018, **134**, 621–631.
18 T. Chen, J. Yu, C. Ma, K. Bikane and L. Sun, *Chemosphere*, 2020, **248**, 125964.
19 K. Pyra, K. A. Tarach, D. Majda and K. Góra-Marek, *Catal. Sci. Technol.*, 2019, **9**, 1794–1801.
20 A. A. Ajibola, J. A. Omoleye and V. E. Efeovbokhan, *Appl. Petrochem. Res.*, 2018, **8**, 211–217.
21 K. A. Tarach, K. Pyra, S. Siles, I. Melián-Cabrera and K. Góra-Marek, *ChemSusChem*, 2018, **12**, 633–638.
22 Y. Li, L. Li and J. Yu, *Chem*, 2017, **3**, 928–949.
23 B. Smit and T. L. M. Maesen, *Nature*, 2008, **451**, 671–678.

3594 | *Catal. Sci. Technol.*, 2024, **14**, 3589–3595

This journal is © The Royal Society of Chemistry 2024

24 S. M. Csicsery, *Zeolites*, 1984, **4**(3), 202–213.

25 W. O. Haag, R. M. Lago and P. B. Weisz, *Faraday Discuss. Chem. Soc.*, 1981, **72**, 317.

26 B. Smit and T. L. M. Maesen, *Chem. Rev.*, 2008, **108**, 4125–4184.

27 N. Katada, K. Suzuki, T. Noda, G. Sastre and M. Niwa, *J. Phys. Chem. C*, 2009, **113**, 19208–19217.

28 J. B. Uytterhoeven, L. G. Christner and W. K. Hall, *J. Phys. Chem.*, 1965, **69**, 2117–2126.

29 F. Yi, Y. Chen, Z. Tao, C. Hu, X. Yi, A. Zheng, X. Wen, Y. Yun, Y. Yang and Y. Li, *J. Catal.*, 2019, **380**, 204–214.

30 M. Ravi, V. L. Sushkevich and J. A. van Bokhoven, *Nat. Mater.*, 2020, **19**, 1047–1056.

31 S. R. Batool, V. L. Sushkevich and J. A. van Bokhoven, *J. Catal.*, 2022, **408**, 24–35.

32 A. Marcilla, M. I. Beltrán and R. Navarro, *Appl. Catal., A*, 2009, **86**, 78–86.

33 S. Kokuryo, K. Miyake, Y. Uchida, S. Tanaka, M. Miyamoto, Y. Oumi, A. Mizusawa, T. Kubo and N. Nishiyama, *ACS Omega*, 2022, **7**, 12971–12977.

34 A. Corma and A. V. Orchillés, *Microporous Mesoporous Mater.*, 2000, **35–36**, 21–30.

35 Z. Dong, W. Chen, K. Xu, Y. Liu, J. Wu and F. Zhang, *ACS Catal.*, 2022, **12**, 14882–14901.

36 S. Kokuryo, K. Tamura, K. Miyake, Y. Uchida, A. Mizusawa, T. Kubo and N. Nishiyama, *Catal. Sci. Technol.*, 2022, **12**, 4138–4144.

37 S. Kokuryo, K. Miyake, Y. Uchida, A. Mizusawa, T. Kubo and N. Nishiyama, *Mater. Today Sustain.*, 2022, **17**, 100098.

38 K. P. de Jong, *Science*, 2016, **351**, 1030–1031.

39 M. Fakhroleslam and S. M. Sadrameli, *Ind. Eng. Chem. Res.*, 2020, **59**, 12288–12303.

40 Y. Wang, Y. Zhang, H. Fan, P. Wu, M. Liu, X. Li, J. Yang, C. Liu, P. Bai and Z. Yan, *Catal. Today*, 2022, **405**, 135–143.

41 S. Vernuccio, E. E. Bickel, R. Gounder and L. J. Broadbelt, *ACS Catal.*, 2019, **9**, 8996–9008.

42 F. Berger and J. Sauer, *Angew. Chem.*, 2021, **133**, 3571–3575.

43 C. Chizallet, C. Bouchy, K. Larmier and L. G. Pirngruber, *Chem. Rev.*, 2023, **123**, 6107–6196.

44 J. Lee, U. G. Hong, S. Hwang, M. H. Youn and I. K. Song, *Fuel Process. Technol.*, 2013, **109**, 189–195.

45 X. Yang, J. Bian, J. Huang, W. Xin, T. Lu, C. Chen, Y. Su, L. Zhou, F. Wang and J. Xu, *Green Chem.*, 2017, **19**, 692–701.

46 J. B. Higgins, R. B. LaPierre, J. L. Schlenker, A. C. Rohrman, J. D. Wood, G. T. Kerr and W. J. Rohrbaugh, *Zeolites*, 1988, **8**, 446–452.

47 J. M. Newsam, M. M. J. Treacy, W. T. Koetsier and C. B. De Gruyter, *Proc. R. Soc. London, Ser. A*, 1988, **420**, 375–405.

48 Z. Kang, X. Zhang, H. Liu, J. Qiu and K. L. Yeung, *Chem. Eng. J.*, 2013, **218**, 425–432.

49 B. Tang, S. Li, W.-C. Song, E.-C. Yang, X.-J. Zhao, N. Guan and L. Li, *ACS Sustainable Chem. Eng.*, 2020, **8**, 3796–3808.

50 X. Yang, Y. Liu, X. Li, J. Ren, L. Zhou, T. Lu and Y. Su, *ACS Sustainable Chem. Eng.*, 2018, **6**, 8256–8265.

51 X. Wang, Y. You, X. Han and X. Jiang, *J. Therm. Anal. Calorim.*, 2022, **147**, 8535–8549.

52 R. Hubesch, Pr. Selvakannan, J. Das, S. Samudrala, K. Foger and S. K. Bhargava, *J. Environ. Chem. Eng.*, 2023, **11**, 110793.

This journal is © The Royal Society of Chemistry 2024

Catal. Sci. Technol., 2024, **14**, 3589–3595 | **3595**